

## Experimental Investigation of Quantum Correlations in a Two-Qutrit Spin System

Yue Fu,<sup>1,2</sup> Wenquan Liu,<sup>1,2</sup> Xiangyu Ye<sup>1</sup>,<sup>1</sup> Ya Wang,<sup>1,2,3</sup> Chengjie Zhang<sup>1,4,5</sup>,  
Chang-Kui Duan<sup>1,2</sup>,<sup>1</sup> Xing Rong,<sup>1,2,3,\*</sup> and Jiangfeng Du<sup>1,2,3,†</sup>

<sup>1</sup>CAS Key Laboratory of Microscale Magnetic Resonance and School of Physical Sciences,  
University of Science and Technology of China, Hefei 230026, China

<sup>2</sup>CAS Center for Excellence in Quantum Information and Quantum Physics,  
University of Science and Technology of China, Hefei 230026, China

<sup>3</sup>Hefei National Laboratory, University of Science and Technology of China, Hefei 230088, China

<sup>4</sup>School of Physical Science and Technology, Ningbo University, Ningbo 315211, China

<sup>5</sup>State Key Laboratory of Precision Spectroscopy, School of Physics and Electronic Science,  
East China Normal University, Shanghai 200241, China



(Received 4 June 2022; accepted 5 August 2022; published 30 August 2022)

We report an experimental investigation of quantum correlations in a two-qutrit spin system in a single nitrogen-vacancy center in diamond at room temperatures. Quantum entanglement between two qutrits was observed at room temperature, and the existence of nonclassical correlations beyond entanglement in the qutrit case has been revealed. Our work demonstrates the potential of the NV centers as the multiqutrit system to execute quantum information tasks and provides a powerful experimental platform for studying the fundamental physics of high-dimensional quantum systems in the future.

DOI: 10.1103/PhysRevLett.129.100501

Quantum correlation sheds light on the most fundamental trait that distinguishes a quantum correlated system from one fully ascribed to a joint classical probability distribution and may reveal the origin of the quantum enhancement in various quantum information tasks [1–4]. Quantum entanglement as a prolonged description of quantum correlation [5], however, has been found to be unable to account for all quantum correlations, leading to the introduction of quantum discord [6,7]. Quantum discord can describe nonclassical correlations even in separable states and may contribute to the quantum enhancement when these states are applied to quantum information processing (QIP) [8–10]. In the last few decades, quantum discord has been studied intensively, but experimental investigations have been limited to qubit systems [11–24]. Recently, researches on  $d$ -level ( $d > 2$ ) systems, hereafter referred to as qudits, are emerging [25–27]. Quantum information processing with qudits may offer higher-dimensional Hilbert space, which results in higher efficiency and flexibility in quantum computing [28,29], larger channel capacity and better noise tolerance in quantum communication [30,31], and relaxed constraints in fundamental tests of the nature [32]. Currently, the experimental studies of quantum correlations in qudit systems have been focused on quantum entanglement [33–37] and quantum steering [38–40]. Quantum discord, a more general description of the quantum correlation, remains untouched experimentally in qutrit systems.

In this paper, we report an experimental investigation of quantum correlations in a two-qutrit system. The

nitrogen-vacancy (NV) center, which has a spin-1 electron spin with the complement of a spin-1 nuclear spin of the  $^{14}\text{N}$  [41], was utilized as a two-qutrit system to study the high-dimensional quantum correlations. The quantum correlations of two-qutrit isotropic states (also known as qutrit Werner states [42]), which are crucial in the research of quantum correlation [5,42–44], were prepared and measured here. The features of quantum discord and quantum entanglement with different values of the state parameter are revealed. It is verified that there is a threshold under which the quantum entanglement vanishes while the quantum discord remains. Such a threshold differs from the one in the case of a two-qubit system [42–45].

The total correlation of a bipartite system  $\rho_{AB}$  quantified by the quantum mutual information [6,7] is defined as

$$I(\rho_{AB}) = S(\rho_A) + S(\rho_B) - S(\rho_{AB}), \quad (1)$$

where  $\rho_A$  ( $\rho_B$ ) is the reduced density matrix of particle  $A(B)$ , and  $S(\rho) = -\text{Tr}[\rho \log_2 \rho]$  is the von Neumann entropy of density matrix  $\rho$ . Both classical and quantum correlations are included in  $I(\rho_{AB})$ . The classical correlation, which depends on the maximum information gained by measuring one particle of the total system, is defined as

$$C(\rho_{AB}) = \max_{B_j^\dagger B_j} \left[ S(\rho_A) - \sum_j q_j S(\rho_A^j) \right], \quad (2)$$

where  $q_j = \text{Tr}[B_j \rho_{AB} B_j^\dagger]$  is the probability of obtaining result  $j$  when performing positive operator-valued measure (POVM)  $\{B_j^\dagger B_j\}$  on subsystem  $B$ , and  $\rho_A^j = \text{Tr}_B[B_j \rho_{AB} B_j^\dagger]/q_j$  is the state of subsystem  $A$  after obtaining outcome  $j$ . Therefore, the difference between the total correlation and the classical correlation given by

$$D(\rho_{AB}) = I(\rho_{AB}) - C(\rho_{AB}) \quad (3)$$

is quantum correlation, which is termed quantum discord.

We focus on a family of qutrit states referred to as isotropic states, which have the form [43]

$$\rho_{\text{iso}} = \frac{(1-p)}{9} \mathbb{I}_3 \otimes \mathbb{I}_3 + p |\psi\rangle\langle\psi|, \quad (4)$$

where  $|\psi\rangle = (|+1, +1\rangle + |0, 0\rangle + |-1, -1\rangle)/\sqrt{3}$  is the maximally entangled state,  $p \in [0, 1]$ , and  $\mathbb{I}_n$  denotes the identity operator in  $n$ -dimensional Hilbert space. Physically, an isotropic state can be regarded as a mixture of the maximally mixed state  $\mathbb{I}_9/9$  and the maximally entangled state  $|\psi\rangle\langle\psi|$  with parameter  $p$  determining the components. Theoretically, there is a threshold  $p_c$  under which the states are separable and otherwise entangled. The threshold varies with the dimension of the isotropic states and  $p_c = 1/4$  for qutrits [43,44]. However, the quantum discord remains nonvanishing for all nonzero  $p$ . Thus, the isotropic states are a representative example of quantum states with zero entanglement nevertheless exhibiting non-zero quantum correlations.

A single negatively charged NV center in [100] face bulk diamond was utilized to investigate the quantum discord and quantum entanglement of a two-qutrit system. The diamond was isotopically purified ( $[^{12}\text{C} = 99.9\%]$ ) to enhance the dephasing time of the electron spin. The NV center consists of a substitutional nitrogen atom adjacent to a carbon vacancy [see Fig. 1(a)]. When an external magnetic field is applied along the NV symmetry axis, the Hamiltonian of the NV center can be written as

$$H_{\text{NV}} = 2\pi(DS_z^2 + \omega_e S_z + QI_z^2 + \omega_n I_z + AS_z I_z), \quad (5)$$

where  $S_z(I_z)$  is the spin operator of the electron (nuclear) spin,  $D = 2.87$  GHz is the electronic zero-field splitting,  $Q = -4.95$  MHz is the nuclear quadrupolar interaction constant, and  $A = -2.16$  MHz is the hyperfine coupling constant.  $\omega_e$  ( $\omega_n$ ) corresponds to the Zeeman frequency of the electron (nuclear) spin. This two-qutrit system contains nine energy levels denoted as  $|m_S\rangle_e|m_I\rangle_n$ , with  $m_S, m_I = 0, \pm 1$  representing the states of the electron and nuclear spins, respectively [see Fig. 1(b)]. For simplicity,  $|m_S\rangle_e|m_I\rangle_n$  is hereafter labeled by  $|m_S, m_I\rangle$ . The magnetic field is set to 500 G, and the NV center is polarized into the state  $|0, +1\rangle$  via applying a 532 nm laser pulse [46]. As shown in Fig. 1(b), microwave (MW) pulses, labeled by

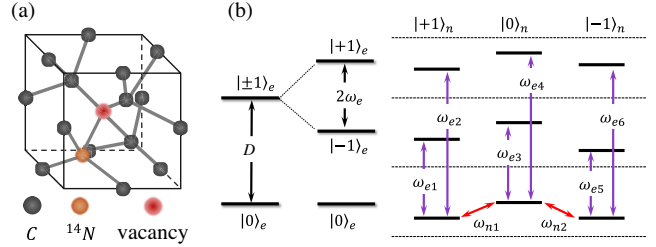


FIG. 1. The two-qutrit system constructed by the NV center. (a) Schematic atomic structure of the NV center. (b) Ground-state energy levels of the NV center. The nine different states of the electron spin and the nuclear spin constitute a two-qutrit system. The transitions between different electron (nuclear) spin states can be steered by microwave (radio frequency) pulses, indicated by purple (red) arrows.

purple arrows, are applied to manipulate the quantum states of the electron spin of the NV center. For the controlling of the nuclear spins, radio frequency (RF) pulses, labeled by red arrows, are utilized.

The Rabi frequency of the electron (nuclear) spin is set to  $\Omega_{\text{MW}} = 0.2$  MHz ( $\Omega_{\text{RF}} = 25$  kHz), as depicted in Fig. 2(a). The relaxation times of both the electron spin and the nuclear spin are measured. For the electron spin, the longitudinal relaxation time is  $T_{1,e} = 4 \pm 1$  ms [Fig. 2(b)] and the dephasing time is  $T_{2,e}^* = 18 \pm 2$   $\mu$ s [Fig. 2(c)]. In Fig. 2(d), we do not see evident decay of the oscillation amplitude during the measurement, which indicates that the dephasing time of the nuclear spin should be much longer than one millisecond. The overall decreasing background probability is caused by the depolarization of the electron spin. The nuclear longitudinal relaxation time  $T_{1,n}$  is estimated to be  $\sim 100$  times  $T_{1,e}$  according to Ref. [47].  $T_{1,n}$ ,  $T_{1,e}$ , and  $T_{2,n}^*$  are much longer than  $T_{2,e}^*$ . Thus, the

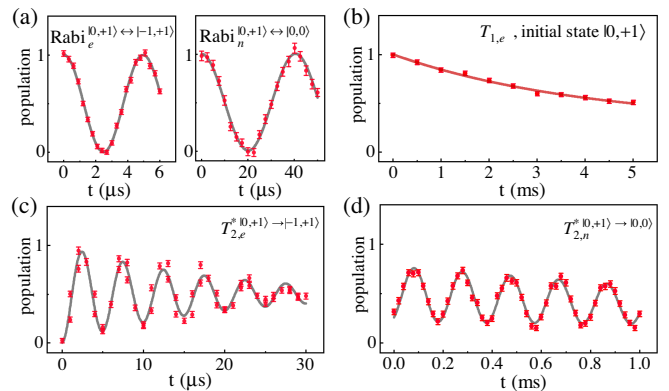


FIG. 2. The properties of the two-qutrit system. (a) Rabi oscillation between different electron (left panel) or nuclear (right panel) spin states. (b) Longitudinal relaxation time of the electron spin  $T_{1,e}$  starting from the state  $|0, +1\rangle$ . (c),(d) Dephasing time of the electron spin and the nuclear spin. All points with error bars are experimental data, and the curves are the fitting results.

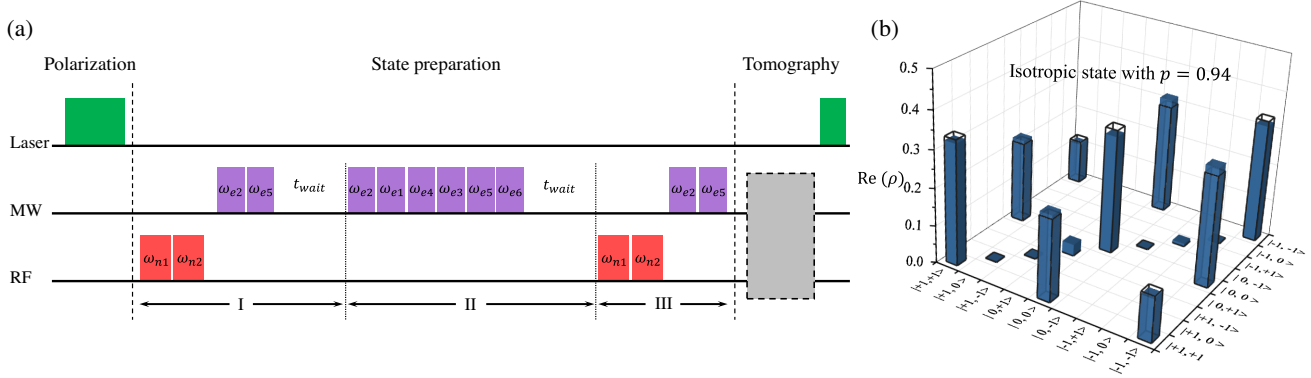


FIG. 3. Experimental pulse sequence and reconstructed density matrix. (a) Diagram of the pulse sequence, which includes polarization, state preparation, and tomography. In the procedure of state preparation, selective MW (purple) and RF (red) pulses are performed to generate the isotropic state  $\rho_{\text{iso}}(p)$ . Frequencies of these pulses correspond to the transition frequencies between energy levels shown in Fig. 1(b). The tomography comprises various measurement sequences to read out different elements of the density matrix (see the Supplemental Material [49] for details). The gray box stands for MW and RF pulses sequences for tomography, which is explained in detail in the Supplemental Material [49]. (b) Experimental density matrix of the entangled state with  $p = 0.94$ . The bars show the experimental outcomes, while wire grids represent corresponding simulation results. Experimental results fit well with simulations, and the state fidelity is 96%.

off-diagonal elements representing the coherence of the electron spin decay much faster than any other elements of the density matrix. The dephasing of the electron spin was the main effect we considered when preparing the isotropic states.

Figure 3(a) shows the diagram of the pulse sequence for studying the quantum correlations of the isotropic states. It consists of three parts: polarization, state preparation, and tomography. The NV center is polarized into the state  $|0, +1\rangle$  via a green laser pulse. The preparation of the isotropic states contains three steps: (I) Applying four selective MW or RF pulses followed by a free evolution time,  $t_{\text{wait}} = 90 \mu\text{s}$ , to prepare the NV center to a mixed state with the form  $\rho_I(p) = P_{+1,+1}^I(p)|+1, +1\rangle\langle +1, +1| + P_{0,0}^I(p)|0, 0\rangle\langle 0, 0| + P_{-1,-1}^I(p)|-1, -1\rangle\langle -1, -1|$ . (II) Applying six selective MW pulses and waiting the same waiting time as in step I to manipulate the system to mixed state  $\rho_{II}(p) = \sum_{i,j=0,\pm 1} P_{i,j}^{II}(p)|i, j\rangle\langle i, j|$ . (III) Applying selective MW and RF pulses to generate the off-diagonal terms of the isotropic states such that  $\rho_{III}(p) = \rho_{\text{iso}}(p)$ . These selective pulses correspond to transitions between different energy levels displayed in Fig. 1(b). The quantum state tomography is performed after the state preparation, and all the nonzero elements of the isotropic states are measured. A maximum likelihood estimation method is utilized to reconstruct the density matrix of the final states [48]. In Fig. 3(b), we show the result of the isotropic state with  $p = 0.94$  as an example. The experimental results (colored bars) fit well with the simulation results (wire grids, with the dephasing noise of the electron spin considered). More details about the state preparation, the measurement sequences, and the state reconstruction can be found in the Supplemental Material [49].

The results of the quantum entanglement and quantum discord measured in our experiment are displayed in Fig. 4. The values of the quantum discord defined by Eq. (3) were obtained from the experimentally reconstructed density matrices using the approach introduced in Ref. [51]. The extremization in Eq. (2) should be taken

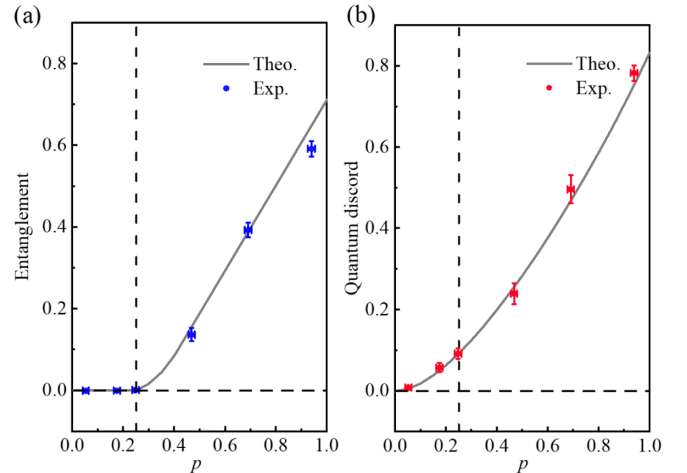


FIG. 4. Quantum correlations of the isotropic states, displaying the experimental results of (a) quantum entanglement and (b) quantum discord. Points denote experimental data, while solid lines show the simulation results. The vertical error bars of the data points were calculated by Monte Carlo simulation with Gaussian statistics. The abscissas of the data points and their error bars were obtained by comparing the experimental results with simulations to find the most likely  $p$  for each Monte Carlo run. Some error bars are smaller than the size of the dots, so they are not visible. The dashed line corresponds to  $p = 1/4$ , which is the dividing line between the separable state and the entangled state.

over all possible complete sets of projective measurements of subsystem  $B$ . We obtained the value of the quantum discord with different measurement bases until it converged. For the isotropic states, the measure of their entanglement can be given by the negativity, defined as  $N(\rho_{\text{iso}}) = (\|\rho_{\text{iso}}^{PT}\|_1 - 1)/2$ , where  $PT$  and  $\|\cdot\|_1$  represent partial transposition and trace norm calculation of the density matrix, respectively [52]. Details about the calculation of the quantum discord and the entanglement are given in the Supplemental Material [49]. Theoretical results in Fig. 4 were obtained by calculating the quantum entanglement and the quantum discord of the simulated states. The experimental results agree well with the theoretical predictions. In the region  $0 < p \leq 1/4$ , the entanglement is zero while the nonzero quantum discord still exists. This unambiguously means a type of quantum correlation beyond quantum entanglement had been experimentally observed in a two-qutrit system. When  $p > 1/4$ , the state has nonzero quantum entanglement and quantum discord that both monotonically increase with  $p$ . Our results show that the qualitative behaviors of the quantum discord and the entanglement in a two-qutrit system are similar to those of a two-qubit system. However, a smaller threshold of the quantum entanglement is observed, as predicted by theories [44,45].

*Discussion.*—Quantum correlation is an essential issue in quantum physics, and recently high-dimensional quantum correlations have aroused tremendous research interest. In this paper, we experimentally studied the quantum correlations between two qutrits in a single NV center. Entanglement in the two-qutrit system has been observed at room temperature, without resorting to cryogenic conditions [36]. In particular, the nonclassical correlations beyond entanglement in the qutrit case are founded. These results show that NV centers are a powerful platform for further investigating the fundamental properties of high-dimensional quantum correlations, such as the essence of quantum correlations [2,8,53] and their relation with quantum superposition and nonlocality [9,10]. Experimentally studying the dynamic behavior of high-dimensional quantum correlations and observing whether there exist sudden death [54] or sudden transition [12] phenomena will also be interesting. Besides this, qutrit systems possess advantages in QIP [27], and experimental investigations of key procedures of QIP [55–57] are necessary. The NV center is a natural high-dimensional system and has a long coherence time even at room temperature. However, it has been utilized as qubits in most studies, which indeed limited its potential. Our work promotes the NV center as a high-dimensional system to execute quantum computation and quantum sensing tasks [25,26,40]. NV qutrit systems may play an important role in high-dimensional quantum information processing, since further coupling two NV centers as qutrits on top of qubits [58–61] is foreseeable, albeit challenging.

This work was supported by the Chinese Academy of Sciences (Grants No. XDC07000000, No. GJJSTD2020001, No. QYZDY-SSW-SLH004, No. QYZDB-SSW-SLH005), Innovation Program for Quantum Science and Technology (Grant No. 2021ZD0302200), the National Key R&D Program of China (Grant No. 2018YFA0306600), the National Natural Science Foundation of China (Grants No. 81788101, No. 11734015), Anhui Initiative in Quantum Information Technologies (Grant No. AHY050000), Hefei Comprehensive National Science Center, the Fundamental Research Funds for the Central Universities, and the open funding program from the State Key Laboratory of Precision Spectroscopy (East China Normal University). X. R. thanks the Youth Innovation Promotion Association of the Chinese Academy of Sciences for the support.

Y. F. and W. L. contributed equally to this work.

\*xrong@ustc.edu.cn

†djf@ustc.edu.cn

- [1] G. Adesso, T. R. Bromley, and M. Cianciaruso, Measures and applications of quantum correlations, *J. Phys. A* **49**, 473001 (2016).
- [2] G. De Chiara and A. Sanpera, Genuine quantum correlations in quantum many-body systems: A review of recent progress, *Rep. Prog. Phys.* **81**, 074002 (2018).
- [3] A. Streltsov, *Quantum Correlations Beyond Entanglement and Their Role in Quantum Information Theory* (Springer, New York, 2015).
- [4] D. Braun, G. Adesso, F. Benatti, R. Floreanini, U. Marzolino, M. W. Mitchell, and S. Pirandola, Quantum-enhanced measurements without entanglement, *Rev. Mod. Phys.* **90**, 035006 (2018).
- [5] R. Horodecki, P. Horodecki, M. Horodecki, and K. Horodecki, Quantum entanglement, *Rev. Mod. Phys.* **81**, 865 (2009).
- [6] H. Ollivier and W. H. Zurek, Quantum Discord: A Measure of the Quantumness of Correlations, *Phys. Rev. Lett.* **88**, 017901 (2001).
- [7] L. Henderson and V. Vedral, Classical, quantum and total correlations, *J. Phys. A* **34**, 6899 (2001).
- [8] E. Knill and R. Laflamme, Power of One Bit of Quantum Information, *Phys. Rev. Lett.* **81**, 5672 (1998).
- [9] K. Modi, A. Brodutch, H. Cable, T. Paterek, and V. Vedral, The classical-quantum boundary for correlations: Discord and related measures, *Rev. Mod. Phys.* **84**, 1655 (2012).
- [10] A. Bera, T. Das, D. Sadhukhan, S. S. Roy, A. Sen De, and U. Sen, Quantum discord and its allies: A review of recent progress, *Rep. Prog. Phys.* **81**, 024001 (2018).
- [11] D. O. Soares-Pinto, L. C. Céleri, R. Aucaise, F. F. Fanchini, E. R. deAzevedo, J. Maziero, T. J. Bonagamba, and R. M. Serra, Nonclassical correlation in NMR quadrupolar systems, *Phys. Rev. A* **81**, 062118 (2010).
- [12] R. Aucaise, L. C. Céleri, D. O. Soares-Pinto, E. R. deAzevedo, J. Maziero, A. M. Souza, T. J. Bonagamba, R. S. Sarthour, I. S. Oliveira, and R. M. Serra, Environment-Induced Sudden Transition in Quantum Discord Dynamics, *Phys. Rev. Lett.* **107**, 140403 (2011).

- [13] A. Singh, Arvind, and K. Dorai, Witnessing nonclassical correlations via a single-shot experiment on an ensemble of spins using nuclear magnetic resonance, *Phys. Rev. A* **95**, 062318 (2017).
- [14] B. P. Lanyon, M. Barbieri, M. P. Almeida, and A. G. White, Experimental Quantum Computing Without Entanglement, *Phys. Rev. Lett.* **101**, 200501 (2008).
- [15] J. S. Xu, X. Y. Xu, C. F. Li, C. J. Zhang, X. B. Zou, and G. C. Guo, Experimental investigation of classical and quantum correlations under decoherence, *Nat. Commun.* **1**, 7 (2010).
- [16] J.-S. Xu, K. Sun, C.-F. Li, X.-Y. Xu, G.-C. Guo, E. Andersson, R. Lo Franco, and G. Compagno, Experimental recovery of quantum correlations in absence of system-environment back-action, *Nat. Commun.* **4**, 2851 (2013).
- [17] G. Adesso, V. D'Ambrosio, E. Nagali, M. Piani, and F. Sciarrino, Experimental Entanglement Activation from Discord in a Programmable Quantum Measurement, *Phys. Rev. Lett.* **112**, 140501 (2014).
- [18] L. T. Knoll, C. T. Schmiegelow, O. J. Farias, S. P. Walborn, and M. A. Larotonda, Entanglement-breaking channels and entanglement sudden death, *Phys. Rev. A* **94**, 012345 (2016).
- [19] M. A. Yurishchev, Quantum discord in spin-cluster materials, *Phys. Rev. B* **84**, 024418 (2011).
- [20] X. Rong, Z. Wang, F. Jin, J. Geng, P. Feng, N. Xu, Y. Wang, C. Ju, M. Shi, and J. Du, Quantum discord for investigating quantum correlations without entanglement in solids, *Phys. Rev. B* **86**, 104425 (2012).
- [21] X. Rong, F. Jin, Z. Wang, J. Geng, C. Ju, Y. Wang, R. Zhang, C. Duan, M. Shi, and J. Du, Experimental protection and revival of quantum correlation in open solid systems, *Phys. Rev. B* **88**, 054419 (2013).
- [22] M. Gessner, M. Ramm, T. Pruttivarasin, A. Buchleitner, H. P. Breuer, and H. Häffner, Local detection of quantum correlations with a single trapped ion, *Nat. Phys.* **10**, 105 (2014).
- [23] A. Abdelrahman, O. Khosravani, M. Gessner, A. Buchleitner, H. P. Breuer, D. Gorman, R. Masuda, T. Pruttivarasin, M. Ramm, P. Schindler, and H. Häffner, Local probe of single phonon dynamics in warm ion crystals, *Nat. Commun.* **8**, 15712 (2017).
- [24] C. J. Wood, M. O. Abutaleb, M. G. Huber, M. Arif, D. G. Cory, and D. A. Pushin, Quantum correlations in a noisy neutron interferometer, *Phys. Rev. A* **90**, 032315 (2014).
- [25] D. Cozzolino, B. Da Lio, D. Bacco, and L. K. Oxenlwe, High-dimensional quantum communication: Benefits, progress, and future challenges, *Adv. Quantum Technol.* **2**, 1900038 (2019).
- [26] Y. Wang, Z. Hu, B. C. Sanders, and S. Kais, Qudits and high-dimensional quantum computing, *Front. Phys.* **8**, 479 (2020).
- [27] M. Erhard, M. Krenn, and A. Zeilinger, Advances in high-dimensional quantum entanglement, *Nat. Rev. Phys.* **2**, 365 (2020).
- [28] H. Wang, J. Qin, X. Ding, M.-C. Chen, S. Chen, X. You, Y.-M. He, X. Jiang, L. You, Z. Wang, C. Schneider, J. J. Renema, S. Höfling, C.-Y. Lu, and J.-W. Pan, Boson Sampling with 20 Input Photons and a 60-Mode Interferometer in a  $10^{14}$ -Dimensional Hilbert Space, *Phys. Rev. Lett.* **123**, 250503 (2019).
- [29] C. Reimer, S. Sciara, P. Roztocki, M. Islam, L. Romero Cortés, Y. Zhang, B. Fisher, S. Loranger, R. Kashyap, A. Cino, S. T. Chu, B. E. Little, D. J. Moss, L. Caspani, W. J. Munro, J. Azaña, M. Kues, and R. Morandotti, High-dimensional one-way quantum processing implemented on  $d$ -level cluster states, *Nat. Phys.* **15**, 148 (2019).
- [30] Y.-H. Luo, H.-S. Zhong, M. Erhard, X.-L. Wang, L.-C. Peng, M. Krenn, X. Jiang, L. Li, N.-L. Liu, C.-Y. Lu, A. Zeilinger, and J.-W. Pan, Quantum Teleportation in High Dimensions, *Phys. Rev. Lett.* **123**, 070505 (2019).
- [31] X.-M. Hu, C. Zhang, B.-H. Liu, Y. Cai, X.-J. Ye, Y. Guo, W.-B. Xing, C.-X. Huang, Y.-F. Huang, C.-F. Li, and G.-C. Guo, Experimental High-Dimensional Quantum Teleportation, *Phys. Rev. Lett.* **125**, 230501 (2020).
- [32] T. Vértesi, S. Pironio, and N. Brunner, Closing the Detection Loophole in Bell Experiments Using Qudits, *Phys. Rev. Lett.* **104**, 060401 (2010).
- [33] M. Kues, C. Reimer, P. Roztocki, L. R. Cortés, S. Sciara, B. Wetzel, Y. Zhang, A. Cino, S. T. Chu, B. E. Little, D. J. Moss, L. Caspani, J. Azaña, and R. Morandotti, On-chip generation of high-dimensional entangled quantum states and their coherent control, *Nature (London)* **546**, 622 (2017).
- [34] J. Wang, S. Paesani, Y. Ding, R. Santagati, P. Skrzypczyk, A. Salavrakos, J. Tura, R. Augusiak, L. Mančinska, D. Bacco, D. Bonneau, J. W. Silverstone, Q. Gong, A. Acín, K. Rottwitt, L. K. Oxenløwe, J. L. O'Brien, A. Laing, and M. G. Thompson, Multidimensional quantum entanglement with large-scale integrated optics, *Science* **360**, 285 (2018).
- [35] L. Lu, L. Xia, Z. Chen, L. Chen, T. Yu, T. Tao, W. Ma, Y. Pan, X. Cai, Y. Lu, S. Zhu, and X.-S. Ma, Three-dimensional entanglement on a silicon chip, *npj Quantum Inf.* **6**, 30 (2020).
- [36] A. Cervera-Lierta, M. Krenn, A. Aspuru-Guzik, and A. Galda, Experimental High-Dimensional Greenberger-Horne-Zeilinger Entanglement with Superconducting Transmon Qutrits, *Phys. Rev. Applied* **17**, 024062 (2022).
- [37] D.-S. Ding, W. Zhang, S. Shi, Z.-Y. Zhou, Y. Li, B.-S. Shi, and G.-C. Guo, High-dimensional entanglement between distant atomic-ensemble memories, *Light. Light.* **5**, e16157 (2016).
- [38] Q. Zeng, B. Wang, P.-Y. Li, and X.-D. Zhang, Experimental High-Dimensional Einstein-Podolsky-Rosen Steering, *Phys. Rev. Lett.* **120**, 030401 (2018).
- [39] Y. Guo, S. Cheng, X. Hu, B.-H. Liu, E.-M. Huang, Y.-F. Huang, C.-F. Li, G.-C. Guo, and E. G. Cavalcanti, Experimental Measurement-Device-Independent Quantum Steering and Randomness Generation Beyond Qubits, *Phys. Rev. Lett.* **123**, 170402 (2019).
- [40] S. Designolle, V. Srivastav, R. Uola, N. H. Valencia, W. McCutcheon, M. Malik, and N. Brunner, Genuine High-Dimensional Quantum Steering, *Phys. Rev. Lett.* **126**, 200404 (2021).
- [41] M. W. Doherty, N. B. Manson, P. Delaney, F. Jelezko, J. Wrachtrup, and L. C. L. Hollenberg, The nitrogen-vacancy colour centre in diamond, *Phys. Rep.* **528**, 1 (2013).

- [42] B. Ye, Y. Liu, J. Chen, X. Liu, and Z. Zhang, Analytic expressions of quantum correlations in qutrit Werner states, *Quantum Inf. Process.* **12**, 2355 (2013).
- [43] B. Baumgartner, B. C. Hiesmayr, and H. Narnhofer, State space for two qutrits has a phase space structure in its core, *Phys. Rev. A* **74**, 032327 (2006).
- [44] E. Chitambar, Quantum correlations in high-dimensional states of high symmetry, *Phys. Rev. A* **86**, 032110 (2012).
- [45] M. Poxleitner and H. Hinrichsen, Gaussian continuous-variable isotropic state, *Phys. Rev. A* **104**, 032423 (2021).
- [46] V. Jacques, P. Neumann, J. Beck, M. Markham, D. Twitchen, J. Meijer, F. Kaiser, G. Balasubramanian, F. Jelezko, and J. Wrachtrup, Dynamic Polarization of Single Nuclear Spins by Optical Pumping of Nitrogen-Vacancy Color Centers in Diamond at Room Temperature, *Phys. Rev. Lett.* **102**, 057403 (2009).
- [47] R. Fischer, A. Jarmola, P. Kehayias, and D. Budker, Optical polarization of nuclear ensembles in diamond, *Phys. Rev. B* **87**, 125207 (2013).
- [48] D. F. V. James, P. G. Kwiat, W. J. Munro, and A. G. White, Measurement of qubits, *Phys. Rev. A* **64**, 052312 (2001).
- [49] See Supplemental Material at <http://link.aps.org/supplemental/10.1103/PhysRevLett.129.100501> for details of the state preparation and reconstruction, experimental procedures, and the calculation of the quantum discord and entanglement, which includes Ref. [50].
- [50] T. Van der Sar, Z. Wang, M. Blok, H. Bernien, T. Taminiau, D. Toyli, D. Lidar, D. Awschalom, R. Hanson, and V. Dobrovitski, Decoherence-protected quantum gates for a hybrid solid-state spin register, *Nature (London)* **484**, 82 (2012).
- [51] R. Rossignoli, J. M. Matera, and N. Canosa, Measurements, quantum discord, and parity in spin-1 systems, *Phys. Rev. A* **86**, 022104 (2012).
- [52] L. Derkacz and L. Jakobczyk, Entanglement versus entropy for a class of mixed two-qutrit states, *Phys. Rev. A* **76**, 042304 (2007).
- [53] E. Biham, G. Brassard, D. Kenigsberg, and T. Mora, Quantum computing without entanglement, *Theor. Comput. Sci.* **320**, 15 (2004).
- [54] M. P. Almeida, F. de Melo, M. Hor-Meyll, A. Salles, S. P. Walborn, P. H. S. Ribeiro, and L. Davidovich, Environment-induced sudden death of entanglement, *Science* **316**, 579 (2007).
- [55] M. A. Yurtalan, J. Shi, M. Kononenko, A. Lupascu, and S. Ashhab, Implementation of a Walsh-Hadamard Gate in a Superconducting Qutrit, *Phys. Rev. Lett.* **125**, 180504 (2020).
- [56] M. Blok, V. Ramasesh, T. Schuster, K. OBrien, J. Kreikebaum, D. Dahlen, A. Morvan, B. Yoshida, N. Yao, and I. Siddiqi, Quantum Information Scrambling on a Superconducting Qutrit Processor, *Phys. Rev. X* **11**, 021010 (2021).
- [57] A. Morvan, V. V. Ramasesh, M. S. Blok, J. M. Kreikebaum, K. O'Brien, L. Chen, B. K. Mitchell, R. K. Naik, D. I. Santiago, and I. Siddiqi, Qutrit Randomized Benchmarking, *Phys. Rev. Lett.* **126**, 210504 (2021).
- [58] M. Pompili, S. L. N. Hermans, S. Baier, H. K. C. Beukers, P. C. Humphreys, R. N. Schouten, R. F. L. Vermeulen, M. J. Tiggelman, L. dos Santos Martins, and B. Dirkse, Realization of a multinode quantum network of remote solid-state qubits, *Science* **372**, 259 (2021).
- [59] F. Dolde, I. Jakobi, B. Naydenov, N. Zhao, S. Pezzagna, C. Trautmann, J. Meijer, P. Neumann, F. Jelezko, and J. Wrachtrup, Room-temperature entanglement between single defect spins in diamond, *Nat. Phys.* **9**, 139 (2013).
- [60] F. Dolde, V. Bergholm, Y. Wang, I. Jakobi, B. Naydenov, S. Pezzagna, J. Meijer, F. Jelezko, P. Neumann, T. Schulte-Herbrüggen, J. Biamonte, and J. Wrachtrup, High-fidelity spin entanglement using optimal control, *Nat. Commun.* **5**, 3371 (2014).
- [61] S. L. N. Hermans, M. Pompili, H. K. C. Beukers, S. Baier, J. Borregaard, and R. Hanson, Qubit teleportation between non-neighbouring nodes in a quantum network, *Nature (London)* **605**, 663 (2022).